

Report Number 11/44

A prototypical model for tensional wrinkling in thin sheets

by

**B. Davidovitch, R.D. Schroll, D. Vella, M. Adda-Bedia, and E.
Cerdeira**



Oxford Centre for Collaborative Applied Mathematics
Mathematical Institute
24 - 29 St Giles'
Oxford
OX1 3LB
England

A prototypical model for tensional wrinkling in thin sheets

B. Davidovitch^{*}, R.D. Schroll^{*}, D. Vella^{†‡}, M. Adda-Bedia[†], and E. Cerda[§]

^{*}Department of Physics, University of Massachusetts, Amherst, MA 01003, [†]Laboratoire de Physique Statistique, Ecole Normale Supérieure, UPMC Paris 06, Université Paris Diderot, CNRS, 24 rue Lhomond, 75005 Paris, France, [‡]OCCAM, Mathematical Institute, 24-29 St Giles', Oxford, OX1 3LB, UK, and [§]Departamento de Física, Universidad de Santiago, Av. Ecuador 3493, Santiago, Chile

Submitted to Proceedings of the National Academy of Sciences of the United States of America

The buckling and wrinkling of thin films has recently seen a surge of interest among physicists, biologists, mathematicians and engineers. This has been triggered by the growing interest in developing technologies at ever decreasing scales and the resulting necessity to control the mechanics of tiny structures, as well as by the realization that morphogenetic processes, such as the tissue-shaping instabilities occurring in animal epithelia or plant leaves, often emerge from mechanical instabilities of cell sheets. While the most basic buckling instability of uniaxially compressed plates was understood by Euler more than 200 years ago, recent experiments on nanometrically thin (ultrathin) films have shown significant deviations from predictions of standard buckling theory. Motivated by this puzzle, we introduce here a theoretical model that allows for a systematic analysis of wrinkling in sheets far from their instability threshold. We focus on the simplest extension of Euler buckling that exhibits wrinkles of finite length - a sheet under axisymmetric tensile loads. This geometry, whose first study is attributed to Lamé, allows us to construct a phase diagram that demonstrates the dramatic variation of wrinkling patterns from near-threshold to far-from-threshold conditions. Theoretical arguments and comparison to experiments show that for thin sheets the far-from-threshold regime is expected to emerge under extremely small compressive loads, emphasizing the relevance of our analysis for nanomechanics applications.

thin film buckling | pattern formation | far from threshold

Thin films are among the ubiquitous examples of flexible structures that buckle under compressive loads. More interestingly, these buckling instabilities usually develop into wrinkled patterns that provide a dramatic display of the applied stress field [1, 2]. Wrinkles align perpendicularly to the compression direction, depicting the principal lines of stress and providing a new geometric tool for mechanical characterization. Traditional buckling theory is regularly used to understand these patterns in the near-threshold (NT) regime, in which the deformations are small perturbations of the initial flat state. However, it has been known since Wagner [3, 4] that when the exerted loads are well in excess of those necessary to initiate buckling, the asymptotic state of the plate is very different from the one observed under NT conditions. In this far-from-threshold (FFT) regime, the stress nearly vanishes in the compression direction and wrinkles mark the region where the compressive stress has collapsed.

Two complementary approaches have provided some insight into wrinkled sheets under FFT loading conditions. In a 1961 paper [5], Stein and Hedgepeth computed the asymptotic stress field in infinitely thin sheets under compression by assuming a vanishing component of the stress tensor along the compression direction. They further showed how such an asymptotic stress field yields the *extent* of wrinkles in several basic examples. A similar formalism that builds on the same assumption was advanced later by Pipkin and coworkers [6]. This approach (often referred to as “tension field” or “relaxed energy” theory) correctly characterizes the stress distribution and the corresponding extent of the wrinkled region, but cannot identify the fine features of the pattern, such as the *wavelength* (or number) of wrinkles, their amplitude,

and the sensitivity to various boundary conditions (BC). A second approach, which does address the wavelength of wrinkled sheets in the FFT regime, has been introduced recently by Cerda and Mahadevan [7], who studied a long rectangular strip under strong uniaxial tension T . Using the simplicity of the stress tensor in this geometry (where the dominant stress component $\approx T$ everywhere) and assuming a balance of bending, compressive and tensile forces, these authors derived an asymptotic scaling law for the FFT wavelength and amplitude of wrinkles. While this idea has been very successful in characterizing the asymptotic wrinkling pattern of tensed rectangular sheets, its implementation in situations characterized by a spatially-varying stress distribution, with a wrinkled state spanning a finite region, remains obscure.

The lack of a theoretical setup that enables a quantitative distinction between wrinkling patterns in the NT and FFT regimes, has led to confusion in interpreting experimental observations. For instance, the length and number of wrinkles in nanofilms have been measured in [8] with high accuracy suggesting that these features could be used as an effective indicator for metrology. In another experiment [9], the onset of wrinkling was identified by slowly increasing the exerted loads or modifying the set-up geometry. These and other experiments have shown various scaling laws for the length and number of wrinkles. However, it is unclear how many *independent* parameters control wrinkling in these systems, what is the structure of the “morphological phase space” spanned by these parameters, and consequently - whether the observed wrinkling patterns reflect NT or FFT conditions.

In this paper we present a FFT theory of wrinkling in very thin sheets that connects the tension field theory [5, 6] to the study of the wrinkle wavelength [7]. The essence of our theory is an expansion of the Föppl–Von Kármán (FvK) equations around the singular limit of a sheet with vanishing bending modulus (the so called “membrane limit” [4]). We show that the extent of the wrinkled region [5] comes from the leading order of that expansion, whereas the wavelength and amplitude of wrinkles [7] result from the sub-leading order. Furthermore, through a quantitative analysis of the FvK equations, our approach enables a clear identification of the NT and FFT regimes of wrinkling patterns, and exposes the subtleties in interpretation of experimental observations. In order to elucidate the basic principles of the theory we focus

Reserved for Publication Footnotes

on a model problem of fundamental interest: a very thin annular sheet under planar axisymmetric loading (Fig. 1). This system, which was apparently first studied by Lamé [10], possess the highest possible symmetry of a two-dimensional (2d) sheet. The instability of such a sheet, which leads to wrinkles of finite extent, may therefore be considered as the simplest extension of Euler's instability (which describes sheets confined in a 1d geometry). Our main findings are summarized in Fig. 2, which presents a schematic phase diagram of wrinkling patterns, ranging from NT to FFT conditions.

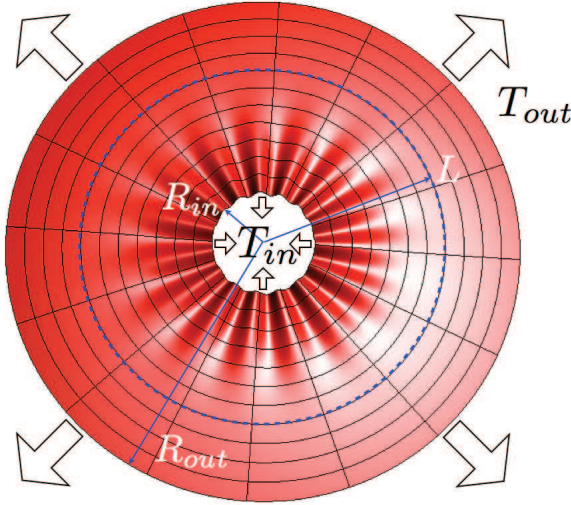


Fig. 1. The Lamé configuration: A mismatch between the inner and outer stresses yields a compression, which is relieved by wrinkling, in the region $R_{in} < r < L$.

We commence by reviewing the classical Lamé solution for the planar state of stretched axisymmetric sheets, and define the *bendability* and *confinement* parameters: ϵ, τ , respectively. Focusing on the high bendability limit ($\epsilon \ll 1$), we show how the Lamé solution gives rise to scaling laws for the threshold confinement $\tau_c(\epsilon)$ at which wrinkling first occurs, and for the extent and number of wrinkles in the NT regime. We then turn to the FFT regime, and introduce the “collapsed compressive stress” assumption that yields the asymptotic FFT stress field. We show how the resulting stress field leads to new scaling laws for the extent and number of wrinkles, which are markedly different from the NT behavior. In the discussion section we describe the general structure of the (ϵ, τ) phase diagram predicted by our results, and address the subtleties of the FvK equations in the FFT regime. We emphasize new insights provided by our model, explain experimental observations and conclude with open questions and future directions.

Near threshold wrinkling

We study the essential differences between the NT and FFT regimes, by focusing on the configuration shown in Fig. 1 where an annular film of inner radius R_{in} and outer radius R_{out} is stretched differentially by radial forces per unit length T_{out} at $r = R_{out}$ and $T_{in} > T_{out}$ at $r = R_{in}$. Similar geometries have been used to study wrinkling under different types of central loads, such as the impact of fast projectiles [11], the deadhesion and wrinkling of a thin sheet loaded at a point [12], and the wrinkling and folding of floating membranes [8, 13]. However, Fig. 1 exhibits the simplest load distribution that leads to wrinkling with finite extent and wavelength.

The planar state. The equilibrium force balance equations are:

$$\partial_r(r\sigma_{rr}) - \sigma_{\theta\theta} + \partial_\theta\sigma_{r\theta} = 0, \quad [1]$$

$$\partial_r(r\sigma_{r\theta}) + \sigma_{r\theta} + \partial_\theta\sigma_{\theta\theta} = 0. \quad [2]$$

The stresses are connected to the radial, hoop and shear strains by Hooke's law $\epsilon_{ij} = [(1 + \nu)\sigma_{ij} - \nu\sigma_{kk}\delta_{ij}]/Y$. Here, $Y = Et$ is the stretching modulus, E is the Young modulus, t the film thickness, and ν is the Poisson ratio. The expressions for the strains in the large deflection limit [4] are:

$$\epsilon_{rr} = \partial_r u_r + \frac{1}{2}(\partial_r \zeta)^2, \quad [3]$$

$$\epsilon_{\theta\theta} = \frac{u_r}{r} + \frac{1}{r}\partial_\theta u_\theta + \frac{1}{2r^2}(\partial_\theta \zeta)^2, \quad [4]$$

$$\epsilon_{r\theta} = \frac{1}{2r}\partial_\theta u_r + \frac{1}{2}\partial_r u_\theta - \frac{1}{2r}u_\theta + \frac{1}{2r}\partial_\theta \zeta \partial_r \zeta, \quad [5]$$

where u_r, u_θ, ζ are, respectively, the radial, azimuthal, and out-of-plane displacements. We included here the shear components, although they will not be required for our analysis. It is a classical problem of linear elasticity [10] to obtain the stress field of the planar, axis-symmetric state: $u_\theta = \zeta = \partial_\theta u_r = 0$, where: $\epsilon_{rr} = \partial_r u_r$, $\epsilon_{\theta\theta} = u_r/r$, $\epsilon_{r\theta} = 0$. Focussing for simplicity on the limit $R_{out} \gg R_{in}$, one finds:

$$\sigma_{rr} = (T_{out} + \Delta T R_{in}^2/r^2); \quad \sigma_{\theta\theta} = (T_{out} - \Delta T R_{in}^2/r^2) \quad [6]$$

where $\Delta T = T_{in} - T_{out}$. In this solution (due to Lamé), the radial stress is tensile everywhere, but if the stress ratio $T_{in}/T_{out} > 2$ the hoop stress becomes compressive for $R_{in} < r < L_{NT}$, where

$$L_{NT} = R_{in} \sqrt{T_{in}/T_{out} - 1}. \quad [7]$$

The existence of compression leads to buckling if the film is thin enough that it becomes energetically favorable to relieve the compressive stress by bending. The Lamé problem is thus characterized by two independent dimensionless groups, *confinement* (τ) and *bendability* (ϵ^{-1}), where:

$$\tau \equiv T_{in}/T_{out}; \quad \epsilon \equiv B/(R_{in}^2 T_{out}) \quad [8]$$

where $B = Et^3/(12(1-\nu^2))$ is the bending modulus. For a given ϵ , buckling is expected if $\tau > \tau_c(\epsilon) > 2$, where $\tau_c(\epsilon)$ is the critical loads ratio. As the sheet gets thinner the energetic cost of bending becomes smaller, hence we expect $\tau_c(\epsilon) \rightarrow 2$ as $\epsilon \rightarrow 0$ (see Fig. 2). Our prime interest is in the high bendability regime, $\epsilon \ll 1$, that describes very thin sheets (alternatively, large tensile loads). For a given $\epsilon \ll 1$ we first consider the NT regime, assuming a loads ratio τ sufficiently close to $\tau_c(\epsilon)$ ¹

Threshold, extent and number of wrinkles. Standard buckling theory in the NT regime consists of a stability analysis of the 1st Föppl–Von Kármán (FvK) equation [4]:

$$B \left[\frac{1}{r} \frac{d}{dr} \left(r \frac{d}{dr} \right) - \frac{m^2}{r^2} \right]^2 f = \sigma_{\theta\theta} \left(-\frac{m^2}{r^2} + \frac{1}{r} \frac{d}{dr} \right) f + \sigma_{rr} \frac{d^2 f}{dr^2} \quad [9]$$

where the out-of-plane displacement is assumed to be $\zeta = f(r) \cos(m\theta)$, and $\sigma_{rr}, \sigma_{\theta\theta}$ assume their Lamé form (6). While the energy and wrinkled extent in the NT regime are determined by Eqs. (6,7), bifurcation analysis (assuming $f(r)$ is infinitesimal¹) yields the value of $\tau_c(\epsilon)$ and the number of wrinkles $m_c(\epsilon)$ of the emerging pattern [14, 15].

¹We assume that the wrinkling instability in the Lamé geometry is *supercritical* (amplitude vanishes at threshold). This assumption implies that $\lim_{\epsilon \rightarrow 0} \tau_c(\epsilon) = 2$ and dictates our NT analysis.

Focusing on the high bendability regime ($\epsilon \ll 1$), a force balance argument yields the NT scaling of $\tau_c(\epsilon)$ and $m_c(\epsilon)$. The forces in Eq. (9) are estimated by using the Lamé solution (6) to approximate the stress in the NT regime: $\sigma_{rr} \approx 2T_{out}$, $\sigma_{\theta\theta} \approx -\tilde{\tau}_c(\epsilon)T_{out}$, where we employed the fact that $\tilde{\tau}_c \equiv \tau_c(\epsilon) - 2 \rightarrow 0$ in this limit¹. Furthermore, the characteristic (radial) scale over which the amplitude $f(r)$ varies is $L_{NT} - R_{in} \approx R_{in} \tilde{\tau}_c(\epsilon)/2$ (see Eq. (7)). These relations allow us to estimate by inspection the different terms in Eq. (9), thus finding that the three dominant forces are associated with azimuthal bending ($\approx Bm_c^4 f/R_{in}^4$), azimuthal compression ($\approx T_{out} \tilde{\tau}_c m_c^2 f/R_{in}^2$), and radial tension ($\approx 2T_{out} f/\tilde{\tau}_c^2 R_{in}^2$). Balancing these forces yields the NT scalings:

$$\tilde{\tau}_c(\epsilon) \sim \epsilon^{1/4} ; m_c(\epsilon) \sim \epsilon^{-3/8} , \quad [10]$$

$$L_{NT}/R_{in} \approx \frac{1}{2} \tilde{\tau}_c(\epsilon) \sim \epsilon^{1/4} . \quad [11]$$

These scaling relations were obtained in [14] by using a non-trivial WKB analysis [14], but to our knowledge the above force balance argument has not been noted before².

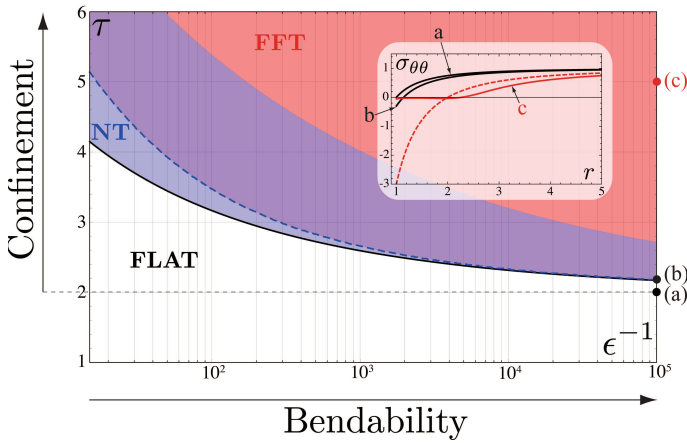


Fig. 2. A schematic phase diagram of wrinkling patterns in the Lamé geometry. The dimensionless parameters ϵ^{-1} , τ represent, respectively, bendability and confinement (see Eq. (8)). Radial wrinkles emerge for $\epsilon, \tau > \tau_c(\epsilon)$ where the threshold curve $\tau_c(\epsilon)$, computed similarly to [14], is marked with a black solid line. The NT analysis is valid below the blue dashed line (see text). After a crossover region (purple) the sheet is under FFT conditions (red). The evolution of the hoop stress as τ increases is shown in the inset for $\epsilon^{-1} = 10^5$ using three curves corresponding to points in the (ϵ, τ) phase space indicated in the main figure. Curves (a) and (b) show the stress profile as predicted by Eq. (6). However, curve (c), which is well within the FFT region, shows that the hoop stress has collapsed in a manner compatible with Eq. (17). To emphasize the collapse of compressive stress, the red dashed line in the inset shows the hoop stress given by Eq. (6) for the same value of τ .

Far From Threshold Wrinkling

Let us turn now to the main focus of our paper: the FFT regime for very thin sheets ($\epsilon \ll 1$). Expecting the NT behavior to characterize a zone in the parameter space (ϵ, τ) above the curve $\tau_c(\epsilon)$ (see Fig. 2), we assume a fixed value of τ sufficiently above this strip, and consider the asymptotic process $\epsilon \rightarrow 0$, keeping τ fixed. This may be achieved, for example, by reducing the sheet thickness while keeping the loads unchanged. We will start by finding the asymptotic FFT stress field, and then show how this stress leads to predictions for the extent L_{FFT} , and number m_{FFT} of wrinkles in this regime.

The asymptotic stress field. Motivated by experiments [8, 9] and following the formalism developed by [3, 5, 6], we assume

that the sheet is composed of two parts: a wrinkled region in $R_{in} < r < L$ with a collapsed hoop and shear stresses $\sigma_{\theta\theta}, \sigma_{r\theta} \rightarrow 0$, and an outer annulus $L < r < R_{out}$ in which the sheet remains planar with stresses following the Lamé form (6) appropriately modified. We shall prove that for $\epsilon \ll 1$ a state with $L > R_{in}$ is energetically favorable compared to the Lamé state, which corresponds to $L = R_{in}$. Thus, wrinkling appears as a mechanism for releasing elastic energy in the film. For $R_{in} < r < L$, Eq. (1) and Hooke's law yield:

$$\sigma_{rr} = T_{in} \frac{R_{in}}{r} ; \epsilon_{rr} = \frac{\sigma_{rr}}{Y} ; \epsilon_{\theta\theta} = -\nu \epsilon_{rr} . \quad [12]$$

Continuity of the radial stress shows that the stresses in the outer annulus have the Lamé form (6) with $R_{in} \rightarrow L$ and $\Delta T \rightarrow \Delta T(L) = T_{in} R_{in}/L - T_{out}$. For a given wrinkle extent L , the FFT stresses are now fully characterized by Eqs. (6,12). Moreover, the radial displacement $u_r(L)$ must also be continuous, and since the Lamé solution at $r \geq L$ implies a link between $u_r(L)$ and $\sigma_{rr}(L)$ one obtains for $r < L$:

$$u_r(r) = R_{in} (T_{in}/Y) \log\left(\frac{r}{L}\right) + u_r(L), \quad [13]$$

with $u_r(L) = [2L(T_{out}/Y) - (1+\nu)R_{in}(T_{in}/Y)]$. The wrinkle extent will be determined by minimizing the energy over L .

Before turning to energy calculations, let us highlight some important aspects of the FFT solution. First, as Eq. (12) indicates, there is pure traction along the radial direction producing a Poisson effect $\epsilon_{\theta\theta} = -\nu \epsilon_{rr} < 0$ in the azimuthal direction and reducing the perimeter at radius r by a total length $-2\pi r \nu T_{in}/Y$. This local contraction shows that for $\nu \neq 0$ the film is not inextensible in the azimuthal direction as was assumed in [7]. However, a similar constraint arises: there is an excess in length when this contraction is not compatible with the geometrical shortening of the perimeter length $2\pi u_r(r)$ that is generated by the inwardly radial displacement $u_r < 0$. In order to reduce stretching energy, this excess of length is relieved by out-of-plane displacement that is highly oscillatory in the azimuthal direction. Using the strain-displacement relations (3,4) and the relation $\epsilon_{\theta\theta} = -\nu \epsilon_{rr}$, we obtain:

$$\int_0^{2\pi} r d\theta [u_r/r + (\partial_\theta \zeta)^2 / (2r^2)] = - \int_0^{2\pi} r d\theta \nu \epsilon_{rr} . \quad [14]$$

Assuming again that $\zeta = f(r) \cos(m\theta)$ ³ one finds:

$$m^2 f^2 / 4r^2 = -u_r/r - \nu \epsilon_{rr} \\ = 2(T_{out}/rY)(R_{in} T_{in}/2T_{out} - L) + R_{in}(T_{in}/rY) \ln(L/r) \quad [15]$$

The positivity of the LHS of Eq. (15) shows that wrinkling is possible only if there is an excess of length of the circle perimeter. An analysis of the RHS of Eq. (15) shows that this is possible for $R_{in} < r < L$ only if $L \leq R_{in} T_{in}/2T_{out}$, thus providing an upper bound for the wrinkled extent.

Finally, let us make two related observations. First, Eq. (15) indicates that the product $m f(r)$ remains finite in the FFT limit, in contrast to the NT regime where $f(r)$ is infinitesimal. Second, Eqs. (4,12,13) imply that the azimuthal variations of the displacement $(\partial_\theta u_\theta)$ are also finite in the FFT

²While the scaling relations for the threshold loads ratio and critical wrinkles number (our Eq. 10) appear in [14] (their Eq. 19), their expression (Eq. 29) corresponding to the NT extent of wrinkles (our Eq. 11) seems to be wrong, as it yields a diverging extent of wrinkles as $R_{out}/R_{in} \rightarrow \infty$.

³Assuming a single-mode shape in the FFT regime is motivated by experiments [8, 9], and simplifies the analysis. There are indications [8] that this assumption fails near a clamped boundary (e.g. $f(r = R_{in}) = 0$), where a wrinkling cascade may emerge, but this does not seem to affect the basic results of our FFT analysis, Eqs. (17,18). Hence, we proceed by assuming a BC's at $r = R_{in}$ that are compatible with Eq. (15). Cascade effects will be mentioned briefly below.

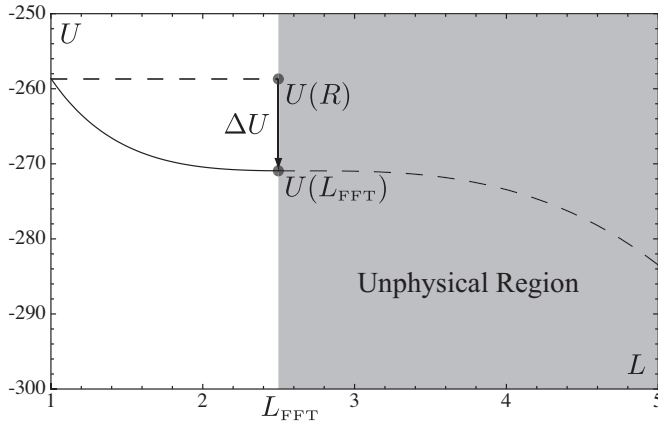


Fig. 3. The mechanical energy U in the FFT limit (normalized by $R_{in}^2 T_{out}^2 / Y$) as a function of the wrinkle extent L (normalized by R_{in}) for $\tau=5$, $R_{out}=10R_{in}$ and $\nu=1/3$. An inflection point exists at $L_{FFT} = \tau/2 = 2.5$. ΔU is the energy gain for $\epsilon \rightarrow 0$ of the FFT energy (inflection point) with respect to the planar, Lamé solution (upper dashed line).

limit⁴. These observations underlie the difference between the singular FFT analysis and the NT behavior which reflects a regular expansion around a planar, axisymmetric state. Indeed, our FFT analysis is based on an asymptotic series in which the expansion parameter is ϵ , in contrast to the NT regime, where the small parameter is the wrinkle amplitude (or equivalently, the distance to threshold $\tau - \tau_c(\epsilon)$).

The extent of wrinkles. In order to determine the wrinkled extent L , we compute the elastic energy $U_E = \frac{1}{2} \int_A dA (\sigma_{rr} \epsilon_{rr} + \sigma_{\theta\theta} \epsilon_{\theta\theta})$ of the FFT stress field. A straightforward calculation using Eqs. (6,12) yields to leading order in $\mathcal{O}(1/R_{out}^2)$:

$$U_E = (\pi/Y) \left\{ (1-\nu)(R_{out}T_{out})^2 + (R_{in}T_{in})^2 \ln(L/R_{in}) + 2(LT_{out} - R_{in}T_{in})^2 - (1-\nu)(R_{in}T_{in})^2 \right\} \quad [16]$$

Note that this energy does not include the costs of bending and out-of-plane stretching of the sheet. We will show below that in the FFT limit these are higher order contributions in ϵ but are nevertheless crucial for obtaining the number of wrinkles m . Since our problem involves constant applied forces at $r = R_{in}, R_{out}$, we must minimize the mechanical energy $U = U_E - W$, where $W = 2\pi[T_{out}R_{out}u_r(R_{out}) - T_{in}R_{in}u_r(R_{in})]$ is the exerted work. Minimizing U as a function of wrinkle extent is analogous to fracture mechanics problems, in which the mechanical energy is minimized as a function of crack length under constant load conditions [16]. Like cracks, wrinkles provide a route for the release of elastic energy. Using a general result from elasticity theory for bodies under constant external loads [16], we find that $W = 2U_E$, and hence $U = -U_E$. In order to minimize U we note that its first derivative $\partial L U = -\pi(2LT_{out} - R_{in}T_{in})^2/(YL) \leq 0$ is zero for:

$$L_{FFT} = R_{in}(T_{in}/2T_{out}). \quad [17]$$

Interestingly, this result coincides with the upper bound implied by the positivity of (15), and also assures continuity of the hoop stress at $r = L_{FFT}$. Thus, energy minimization naturally yields a value for the stress at the tip of the wrinkles that smoothly matches the flat region in the film to the wrinkled one. Fig. 3 shows that Eq. (17) corresponds to an inflection point of U , but the upper bound found above guarantees that this is the actual length in the FFT limit. Fig. 3 also indicates that at the FFT limit, the energy at the inflection point

$U(L_{FFT})$ is lower than the Lamé value $U(R_{in})$. Thus, for $\tau > 2$ and sufficiently small ϵ , there indeed is an energy gain in the FFT regime, with respect to the planar state (Lamé value). Eq. (17) is one of the central results of our analysis. It reflects a linear scaling of the extent of the wrinkles in the FFT regime with the ratio T_{in}/T_{out} , in sharp contrast to the square root scaling that characterizes the NT limit, Eq. (7).

Number of wrinkles. As noted already, our FFT theory amounts to an asymptotic expansion of the FvK equations around the “membrane limit”. We determined above the wrinkle extent from the leading order in this expansion, whose energetic contribution (16) asymptotes to a finite value as $\epsilon \rightarrow 0$. This leading order is insensitive, however, to the fine features of the pattern, most importantly the number of wrinkles. In order to determine the number of wrinkles we turn now to the next (subdominant) order in the expansion, whose energetic contribution will be shown to be $\sim \sqrt{\epsilon}$.

While Eq. (15) reveals that the product $mf(r)$ must remain finite, we expect $|f|$ to become smaller and hence m to diverge as $\epsilon \rightarrow 0$. This agrees with experimental observations [7, 8]. It is also correlated with the fact (similar to the NT regime) that the out-of-plane forces dominating the 1st FvK Eq. (9) in the FFT regime are azimuthal bending ($\approx Bm^4 f/L_{FFT}^4$), azimuthal compression ($\approx \sigma_{\theta\theta} m^2 f/L_{FFT}^2$) and radial stretching ($\approx \sigma_{rr} f/L_{FFT}^2$, with σ_{rr} given by (12)). Notice that in contrast to the NT analysis, the FFT force estimates assume the limit $\epsilon \rightarrow 0$ while keeping the loads ratio τ at a fixed value (and hence, by Eq. 17, fixing L_{FFT}/R_{in}), and allows the value of $\sigma_{\theta\theta}$ to vary. Balance of these three forces implies the hoop stress scaling $\sigma_{\theta\theta} \sim \sqrt{BT_{out}/R_{in}}$. This result can be expressed as $\sigma_{\theta\theta}/T_{out} \sim \epsilon^{1/2}$, whereas the NT result, Eq. (10) yields $\sigma_{\theta\theta}/T_{out} \sim \epsilon^{1/4}$. Both scalings show that for small ϵ , small compressive loads are required to buckle the film. More interestingly, they express the essence of the transition from NT to FFT conditions: A rapid collapse of the compressive stress as the loads ratio is increased beyond threshold (for a fixed, small ϵ). The same force balance implies the FFT scaling of the number of wrinkles:

$$m \sim k(\tau)(R_{in}^2 T_{out}/B)^{1/4} \sim \epsilon^{-1/4} \quad [18]$$

for some $k(\tau)$, in sharp contrast to the NT scaling (10). This scaling has already been predicted in [7], and is supported by experiments on ultrathin sheets, where ϵ is estimated to be below 10^{-6} [8]. Computing the value of the pre-factor $k(\tau)$ introduces complexities that will be explained later on.

Discussion

The phase space structure. Focusing on highly bendable sheets ($\epsilon \ll 1$), our analysis of the NT and FFT regimes yields the schematic phase diagram, Fig. 2. Once the external loads induce sufficient compressive hoop stress, a wrinkled shape will emerge. Here the threshold line was obtained from a linear analysis similar to Ref. [14] (albeit with a free edge BC at $r = 1$ to eliminate a spurious boundary layer near $r = 1$).

The stress field and pattern features must change markedly as the loads ratio τ is increased above threshold. Most importantly, the compressive hoop stress decreases (from $O(\epsilon^{1/4})$ to $O(\epsilon^{1/2})$), the extent of wrinkles increases (from $O(\epsilon^{1/4}R_{in})$ to $R_{in}\tau/2$), and the number of wrinkles decreases (from $O(\epsilon^{-3/8})$ to $O(\epsilon^{-1/4})$). It is interesting that this rather nontrivial (and arguably, nonintuitive) behavior follows

⁴ The fact that $\partial_\theta u_\theta$ remains finite in the FFT limit explains why the nonlinear model of [9], that assumes negligibility of this and similar terms, cannot describe this regime

directly from the force balance (FvK) equations for thin sheets supplemented by two rather intuitive assumptions. Firstly, we assume the collapse of the compressive stress in the FFT regime. Secondly, we assume that the normal force balance (1st FvK equation) in highly bendable sheets is dominated by three forces: bending and compression in the azimuthal (transverse to wrinkles) direction and stretching in the radial (along wrinkles) direction. This balance, which explicitly requires the shape to be curved in both spatial directions (and hence precludes translation invariance), underlies the morphological complexity of the planar, axisymmetric Lamé problem, a complexity that is absent in the simpler classical Euler buckling of a sheet confined in 1d geometry.

The existence of clearly distinguished NT and FFT patterns prompts a very practical question: How large is the NT regime that is described by traditional post-buckling theory? Specifically, consider a sheet with fixed thickness, geometry, and external load (hence fixed ϵ) and assume the loads ratio τ is increased above the threshold value $\tau_c(\epsilon)$. We ask two related but distinct questions: First - at what value of τ should we expect to observe significant deviations from the NT behavior (Eqs. 10,11)? Second - at what value of τ should we begin to observe features of the FFT pattern (Eqs. 17,18)? The first question can be addressed through a perturbation theory (in the amplitude $|f|$), by estimating the characteristic value of τ where the perturbed stress values become comparable to the pre-buckled Lamé stresses, Eq. (6). We find that the width of the NT region shrinks at a rate $\sim \epsilon^{1/2}$ (dashed blue curve in Fig. 2). The second question is more subtle. Our asymptotic analysis of the FFT regime, which considers the limit $\epsilon \rightarrow 0$ for a fixed value $\tau > 2$, shows that FFT behavior is expected to emerge above a crossover regime whose size shrinks with ϵ (the purple region in Fig. 2). However, our analysis is insufficient to predict the actual size of the crossover zone, nor can it reveal the exact nature of the NT-FFT transition. The above discussion motivates the search for a nonlinear model of the Lamé problem, that will simplify the full FvK equations, and will capture the behavior of wrinkling patterns for all values of ϵ and $\tau > \tau_c(\epsilon)$.

The predicted narrowing of the NT regime (and transition to FFT) in the limit $\epsilon \rightarrow 0$, indicates that experiments would need to be constructed extremely carefully in order to observe the NT regime for highly bendable sheets.

FFT analysis of the FvK equations. While the NT analysis amounts to a regular perturbation around the planar state [14, 15], our FFT analysis introduces an expansion of the FvK equations around the singular “membrane limit” $\epsilon = 0$. The singular nature of the FFT expansion is further clarified by considering the energy. The leading energy $U \sim (R_{in}T_{out})^2/Y$, Eq. (16), approaches a finite (τ -dependent) value as $\epsilon \rightarrow 0$. This value determines the extent of wrinkles but does not involve their number. By contrast, the subleading energy involves terms such as the bending energy $U_B = 2\pi(B/4) \int_{R_{in}}^L dr m^4 f^2(r)/r^3$ which scales as $\sim \epsilon^{1/2}U$ and hence vanish as $\epsilon \rightarrow 0$. However, despite its apparent negligibility, the sub-dominant energy involves m , and hence it selects the number of wrinkles. In this respect, our FFT theory joins two apparently distinct ideas: The approach of [5, 6, 4], which yields the asymptotic stress field with collapsed compressive stress and consequently the extent of the wrinkles (17), and the approach of [7] which yields the asymptotic scaling of the number of wrinkles (18). Our asymptotic expansion of the FvK equations, which considers the thin-sheet limit $\epsilon \rightarrow 0$ for a fixed $\tau > \tau_c(\epsilon)$, shows that these two approaches are complementary: The first results from the leading order, whereas the second emanates from the next (sub-leading) or-

der of the expansion. The unusual link between the leading and sub-leading orders is manifested in Eq. (15), which expresses a constraint on fine features of the pattern (i.e. the product $m f(r)$) imposed by the FFT stress field. One should notice that phenomena in which macro-scale features are dominated by a leading energy and fine features are governed by a sub-leading energy, are not unique to elastic sheets. A representative example is the domain structure in the intermediate state of a type-I superconductor [17].

An important consequence of the above discussion pertains to the robustness of patterns in the FFT regime. The small ratio $\epsilon^{1/2}$ between the sub-leading and leading energies suggests that the wrinkle extent is more robust than the wavelength. This is manifested when studying the effect of clamped BC's ($f(r = R_{in}) = 0$) on the wrinkling pattern³. While the dominant energy and hence the extent of wrinkles, Eq. (17), are indifferent to this effect, similar arguments to those underlying Eq. (18) show that a smooth (tension-dominated) wrinkling cascade that emerge near the clamped edge [18] may strongly modify the pre-factor $k(\tau)$ in Eq. (18).

Another manifestation of the subtlety of our FFT expansion is found when attempting to compute the pre-factor $k(\tau)$ in the scaling law (18). To this end (regardless of the assumed BC's at $r = R_{in}$), we must use Eqs. (12,13,15) to compute the bending energy U_B and the out-of-plane stretching energy $U_S = 2\pi(1/4) \int_{R_{in}}^L dr r \sigma_{rr}(r) f'(r)^2$ as functions of m , and determine m as the minimizer of these sub-dominant energies. We find, however, a divergence of $f'(r)$ and U_S as $L \rightarrow L_{FFT}$ for all m . Initially, this observation can raise doubts to the validity of our theory. However, careful consideration reveals the source of this divergence: our matching conditions at $r = L$ assume a direct transition from the planar state at $r > L$ to the collapsed compressive stress region at $r < L$. The divergence of U_S can be remedied if the unphysical “pointwise” matching is replaced by a smooth matching of the two regions. The subtle aspects of our analytic approach emphasize once more the necessity of developing model equations that will enable effective and accurate numerical study of wrinkling patterns in the whole (ϵ, τ) phase space.

Comparison to previous experiments. There are many papers that describe wrinkling phenomena under various geometries and load configurations. The distinction we have drawn here between wrinkling in the NT and FFT regimes is crucial for obtaining a proper understanding of these experiments. We restrict the following discussion to two papers that address thin sheets in configurations similar to the Lamé geometry.

In the experiments of [8], a very thin circular sheet (t ranging from 30 – 300 nm) floats on water and hence is subject to a surface tension $T_{out} = \gamma$ at its perimeter $r = R_{out}$. A liquid drop is placed at the center, deforming the sheet beneath it, and exerting an in-plane tensile force T_{in} at the contact line $r = R_{in}$. The problem is thus analogous to the Lamé problem, but determining T_{in} is a subtle problem that has not yet been fully resolved [19]. Typical values of ϵ are less than 10^{-6} , and hence our thin sheet analysis seems relevant. The number of wrinkles (Fig. 2 of [8]) shows excellent agreement with the FFT scaling (18), indicating that the experiment corresponds to FFT conditions and that the pre-factor $k(\tau)$ in Eq. (18) is nearly constant within the range of loads ratios studied. Since T_{in} is unknown, our result (17) cannot be directly compared to the experiments of [8]. Nevertheless, it does resolve a puzzle raised by their empirical observation that the length of wrinkles $\approx C_L \sqrt{Y/\gamma} R_{in}$, with C_L a numerical constant. The authors of [8] assumed the NT scaling, Eq. (7), and concluded that their results indicate that T_{in} is “independent of surface tension, which is implausible”. However, the FFT

scaling, Eq. (17), shows that the empirical law is consistent with $T_{in} \sim \sqrt{Y\gamma}$, suggesting instead that the in-plane tension exerted by the drop at the contact line is affected “equally” by the surface tension and the stretching modulus.

In contrast to [8], the Lamé geometry was studied in [9] by mechanically stretching an annular sheet in an axisymmetric fashion⁵. We find that the parameter values reported in [9] correspond to a small characteristic value of $\epsilon \lesssim 10^{-3}$, but note that the studied range of $\log(\epsilon)$ is significantly narrower than in [8] and therefore comparison to the predicted scaling laws is less conclusive. Let us discuss first Fig. 8 of [9], which provides a striking insight into a subtle aspect of wrinkling patterns. The pattern amplitude is plotted there as a function of the control parameter δ_i (that is proportional to τ ⁵) and exhibits a square-root dependence, $|f| \sim \sqrt{\tau - \tau_c}$, which is a universal feature of patterns in the NT regime¹. However, analysis of our Eq. (15) for $L = L_{FFT}$ and small values of $\tau - 2$ shows that, surprisingly, the same square-root dependence characterizes the FFT regime. Thus, while the stress distribution, as well as the extent and number of wrinkles strongly vary between the NT and FFT regimes, the pattern amplitude does not disclose this dramatic change. Another central result of [9] is presented in their Fig. 7, where the number of wrinkles m is shown to scale linearly with R_{in} , in apparent contradiction with both the NT ($m \sim \epsilon^{-3/8}$, (11)) and the FFT ($m \sim \epsilon^{-1/4}$, (18)) scalings. However, re-plotting the data on a log-log scale, we find the relation $m \sim \epsilon^{-c}$, where c ranges from 0.25 – 0.4. This large uncertainty does not allow a clear distinction between NT and FFT behaviors, and emphasizes the necessity of a large interval of $\log(\epsilon)$ values for analyzing wrinkling patterns in thin sheets.

Conclusions

Our paper carries two central messages: First - wrinkles in very thin sheets may appear as two distinct types of patterns, near-threshold (NT) and far-from-threshold (FFT). In each of these regimes different asymptotic relations characterize the morphology and stress field. Second - while the NT regime can be described with the standard post-buckling approach, analysis of the FFT regime requires a nonstandard perturbation theory around the singular “membrane limit”. This analysis makes direct use of the collapse of compressive stress in this limit. Our FFT theory unifies the stress field analysis

of [5] and the scaling ideas of [7]. We have demonstrated the FFT theory for the Lamé problem - a sheet of axisymmetric geometry and loads, which is the simplest extension of the classical Euler buckling of sheets confined in a 1d geometry. Our analysis makes use of the high degree of symmetry of the Lamé problem, which implies dependence of the patterns on two dimensionless parameters (ϵ, τ) only. Nevertheless, we anticipate that the method introduced here will lead to insights on wrinkling phenomena in set-ups with a lower level of symmetry (for instance, the indentation experiments of [13]).

Our analysis substantiates the analogy discovered by Mansfield between crumpling and wrinkling [4, 20]. Similarly to our wrinkling pattern, the macro-scale features of a crumpled shape are determined by minimizing a dominant energy [21]. However, while the dominant energy of a wrinkling pattern consists of stretching (Eq. 16), a crumpling pattern is dominated by a bending energy, whose minimization leads to a stress focusing shape: line or point singularities that connect strainless regions. Furthermore, in both cases the sub-dominant energies consist of a mixture of stretching and bending terms that determine small-scale features of the pattern: wavelength (wrinkling) and the size of stress-focusing zones (crumpling). Recent experiments [22, 23] have shown that this mixture of sub-dominant energies leads to the complex shapes of curtains: multi-scale, hierarchical patterns that interpolate between crumpling-like and wrinkling-like shapes.

The classification of wrinkling patterns into NT and FFT regimes provides new insights into the behavior of elastic sheets. It also raises some interesting problems concerning the nature of the transition between the NT and FFT regimes and crucial aspects of the FFT analysis, such as the computation of the exact wrinkle number, and how it is influenced by boundary conditions. We hope that the ideas introduced in this paper will inspire theoretical and experimental works that will further elucidate the subtleties of wrinkling phenomena and other types of deformations of thin compressed sheets.

ACKNOWLEDGMENTS. We thank P. Bela, R. Kohn and N. Menon for useful discussions. We acknowledge support by the Petroleum Research Fund of ACS (B.D.) and NSF-MRSEC on Polymers at UMass (R.S.). This publication is based on work supported in part by grant No. KUK-C1-013-04 made by King Abdullah University of Science and Technology (D.V.). M.A.B. and E.C. acknowledge the support of CNRS-Conicyt 2008. E.C. thanks Fondecyt project 1095112 and Anillo Act 95. We thank the Aspen Center for Physics for hospitality during the final stages of this work.

1. Bowden N et al. (1998) Spontaneous formation of ordered structures in thin films of metals supported on an elastomeric polymer. *Nature* 393: 146-149.
2. Genzer J, Groenewold J (2006) Soft matter with hard skin: From skin wrinkles to templating and material characterization. *Soft Matter* 2: 310-323.
3. Wagner H (1929) Ebene Blechwandtrger mit schr dnnem Stegblech. *Z. Flugtechn. Motorluftschiffahrt* 20: 8-12.
4. Mansfield E-H (1989) *The Bending and Stretching of Plates*. Cambridge University Press, Cambridge.
5. Stein M, Hedgepeth J-M (1961) Analysis of partly wrinkled membranes. *NASA Technical Note D-813*.
6. Pipkin A-C (1986) The relaxed energy density for isotropic elastic membranes. *IMA J. App. Math.* 36:85-99.
7. Cerda E, Mahadevan L (2003) Geometry and physics of wrinkling. *Phys. Rev. Lett.* 90:074302; Cerda E, Ravi-Chandar K, Mahadevan L (2002) Thin films - Wrinkling of an elastic sheet under tension. *Nature* 419: 579-580.
8. Huang J et al. (2007) Capillary wrinkling of floating thin polymer films. *Science* 317:650-653.
9. Géminard J-C, Bernal R, Melo F (2004) Wrinkle formations in axi-symmetrically stretched membranes. *Eur. Phys. J. E* 15:117-126.
10. Timoshenko S-P, Goodier J-N (1970) *Theory of Elasticity*. McGraw Hill.
11. Vermorel R, Vandenbergh N, Villermaux E (2009) Impacts on thin elastic sheets. *Proc. R. Soc. Lond. A* 465:823-842.
12. Chopin J, Vella D, Boudaoud A (2008) The liquid blister test. *Proc. R. Soc. Lond. A* 464:2887-2906.

13. Holmes D-P, Crosby A-J (2010) Draping Films: A Wrinkle to Fold Transition. *Phys. Rev. Lett.* 105:038303.
14. Coman C-P, Bassom A-P (2007) On the wrinkling of a pre-stressed annular thin film in tension. *J. Mech. Phys. Solids* 55:1601-1617.
15. Adams G-G (1993) Elastic wrinkling of a tensioned circular plate using VonKarman plate-theory. *J. App. Mech.* 60:520-525.
16. Lawn B (2004) *Fracture of Brittle Solids*. Cambridge University Press, 2nd ed., Cambridge.
17. Choksi R, Kohn R-V, and Otto F (2004) Energy minimization and flux domain structure in the intermediate state of a type-I superconductor. *J. Nonlinear Science* 14:119-171.
18. Davidovitch B (2009) Period fissioning and other instabilities of stressed elastic membranes. *Phys. Rev. E* 80:025202(R).
19. Vella D, Adda-Bedia M, Cerda E (2010) Capillary wrinkling of elastic membranes. *Soft Matter* 6:5778-5872.
20. Mansfield E-H (1968) *Tension Field Theory, A New Approach Which Shows Its Duality With Inextensional Theory*. *Proc. XII Int. Cong. App. Mech.* 305-320.
21. Witten T-A (2007), Stress Focusing In Elastic Sheets. *Rev. Mod. Phys.* 79:643-675.
22. Huang J. et al. (2010) Smooth Cascade of Wrinkles at the Edge of a Floating Elastic Film. *Phys. Rev. Lett.* 105:038302.
23. Vandeparre H et al. (2011) Wrinkling Hierarchy in Constrained Thin Sheets from Suspended Graphene to Curtains. *Phys. Rev. Lett.* 106:224301.

⁵ The control parameters in [9] were R_{in} (their r_0), $u_r(R_{out})$ (their β), and the “access” radial displacement at R_{in} (their δ_i). Hence, the tensions T_{in} and T_{out} are proportional to the thickness. Using Eqs (3.6) and Hooke’s law, we find $\tau = 2R_{out}/12(1+\nu)R_{in}^2\beta$, and $\tau = \delta_i R_{out}(1-\nu)/\beta R_{in}(1+\nu)$. The last relation corresponds to the NT regime which is sufficient for our discussion, but is different in the FFT regime. The sheet thickness in [9] was $t = 0.2$ mm, and $R_{out}/R_{in} \geq 6$.

RECENT REPORTS

21/11	A novel model for one-dimensional morphoelasticity. Part I: Theoretical foundations	Hall Menon McCue McElwain
22/11	A novel model for one-dimensional morphoelasticity. Part II: Application to the contraction of fibroblast-populated collagen lattices	Hall Menon McCue McElwain
23/11	Positive or negative Poynting effect? The role of adscititious inequalities in hyperelastic materials	Mihai Goriely McCue McElwain
24/11	On approaches to modelling lattice dislocations	Hall Markenscoff
25/11	Nonlinear waves in heterogeneous elastic rods via homogenization	de Luna Emptage Goriely Bressloff
26/11	Synaptic bistability due to nucleation and evaporation of receptor clusters	Burlakov Duričković Goriely
27/11	Particle trapping and banding in rapid solidification	Elliot Peppin
28/11	Growth of confined cancer spheroids: a combined experimental and mathematical modelling approach	Loessner Flegg Byrne Hall Moroney Clements McElwain Hutmacher
29/11	Floating carpets and the delamination of elastic sheets	Wagner Vella
30/11	Numerical Study of Liquid Crystal Elastomers by a Mixed Finite	Luo Calderer
31/11	The indentation of pressurized elastic shells: From polymeric capsules to yeast cells	Vella Ajdari Vaziri Boudaoud
32/11	Wrinkling of pressurized elastic shells	Vella Ajdari Vaziri Boudaoud
33/11	Data assimilation using bayesian filters and B-spline geological models	Duan Farmer Hoteit Lu

36/11	A simple mathematical model for investigating the effect of cluster roots on plant nutrient uptake	Zygalakis Roose
37/11	Frequency jumps in the planar vibrations of an elastic beam	Neukirch Frelat Goriely Maurini
38/11	Ice-lens formation and con- nemenent-induced supercooling in soils and other colloidal materials	Style Cocks Peppin Wettlaufer
39/11	An asymptotic theory for the re-equilibration of a micellar surfac- tant solution	Griffiths Bain Breward Chapman Howell Water
40/11	Higher-order numerical methods for stochastic simulation of chemical reaction systems	Székelly Burrage Erban Zygalakis
41/11	On the modelling and simulation of a high pressure shift freezing process	Smith Peppin Ángel M. Ramos
42/11	An efficient implementation of an implicit FEM scheme for fractional-in-space reaction-diffusion equations	Burrage Hale Kay
43/11	Coupling fluid and solute dynamics within the ocular surface tear film: a modelling study of black Line osmolarity	Zubkov Breward Gaffney

**Copies of these, and any other OCCAM reports can be obtained
from:**

**Oxford Centre for Collaborative Applied Mathematics
Mathematical Institute
24 - 29 St Giles'
Oxford
OX1 3LB
England
www.maths.ox.ac.uk/occam**